Reliable and unreliable dynamics in driven coupled oscillators

Kevin K. Lin, Eric Shea-Brown, and Lai-Sang Young
Courant Institute of Mathematical Sciences and Center for Neural Science
New York University
(Dated: August 8, 2006)

This letter concerns the *reliability* of coupled oscillator networks in response to fluctuating inputs. Reliability means that (following a transient) an input elicits identical responses upon repeated presentations, regardless of the system's initial condition. Here, we analyze this property for *two coupled oscillators*, demonstrating that oscillator networks exhibit both reliable and unreliable dynamics for broad ranges of coupling strengths. We further argue that unreliable dynamics are characterized by strange attractors with random SRB measures, implying that though unreliable, the responses lie on low-dimensional sets. Finally, we show that 1:1 phase locking in the zero-input system corresponds to high susceptibility for unreliable responses. A geometric explanation is proposed.

For a dynamical system, the question of reliability can be formulated as follows: if an external stimulus is applied multiple times, will it elicit essentially the same response each time *independent of the state of the system* when the input is received? The answer is fundamental to the ability of the system to encode stimuli in a repeatable way. It also determines if an ensemble of such systems would synchronize if they receive the signal as a common input. Applications range from biological pacemakers to laser arrays to neurons processing incoming stimuli [1].

The reliability of isolated oscillators has been explored extensively in both experiment and theory. For example, single neurons respond reliably to fixed-current signals in laboratory experiments [2]. Theoretical studies [3, 4] have shown that reliability is typical for phase oscillator models, *i.e.* ODEs on the circle. Unreliable dynamics, characterized by an apparently chaotic response to the stimulus, have been shown to occur if the state space of the oscillator has more than one dimension and the stimulus is sufficiently strong [5].

The reliability of *networks* of coupled oscillators is far less well understood. Here, we take a first step toward understanding how input stimulus and network architecture interact to determine reliability. For concreteness, we focus on a 2-oscillator pulse-coupled network.

Our main findings are: (1) Single oscillators that are reliable in isolation can become highly unreliable when coupled, depending on input amplitude and coupling strengths. **(2)** Strange attractors with random SRB measures are a signature of unreliability. The singularity of these measures implies that even in unreliable dynamics, phase relations are highly structured. **(3)** Parameters at which the two-cell network is especially susceptible to producing unreliable dynamics coincide with the onset of 1:1 phase locking for the system with zero input. Geometric explanations for some of the observed phenomena are proposed.

I. THE TWO-CELL MODEL

We consider in this letter a 2-cell network of oscillators with the following structure:

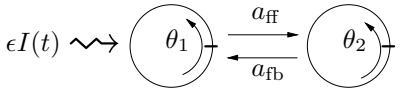

To illustrate our ideas, we use a standard phase model which characterizes the dynamics of limit cycle oscillators with smooth, pulsatile interactions [6]:

$$\begin{aligned}\dot\theta_1 &= \omega_1 + a_{\rm fb} g(\theta_2) z(\theta_1) + \epsilon z(\theta_1) I(t) \\ \dot\theta_2 &= \omega_2 + a_{\rm ff} g(\theta_1) z(\theta_2),\end{aligned} \tag{1}$$

The state of each oscillator is described by a phase, i.e., an angular variable $\theta_i \in \mathbb{S}^1 \equiv \mathbb{R}/\mathbb{Z}, i = 1, 2$. The constants ω_1 and ω_2 are the cells' intrinsic frequencies, $I(t)$ is the external stimulus and ϵ its amplitude. In this letter $I(t)$ is taken to be white noise. The coupling is via a "bump function" g which vanishes outside of an interval $(-b, b)$; we have taken b to be ≈ 0.05. On $(-b, b)$, g is smooth, it is ≥ 0 and satisfies $\int_{-b}^{b} g(\theta)\, d\theta = 1$. The meaning of g is as follows: We say the ith oscillator "spikes" when $\theta_i(t) = 0$. Around the time that an oscillator spikes, it emits a pulse which modifies the other oscillator. The strength of the feedforward (ff) coupling is given by $a_{\rm ff}$ ("forward" refers to the direction of stimulus propagation), and likewise for $a_{\rm fb}$, the feedback connection. Finally, the response of an oscillator to coupling and stimulus is modulated by its phase response curve z [7, 8]. We take $z(\theta) = \frac{1}{2\pi}(1 - \cos(2\pi\theta))$, characterizing oscillators near saddle-node bifurcations on limit cycles (as for many neuron models [8]).

The simplest way to investigate the reliability of a system is to carry out many simulations, using a different initial condition each time but driving the system with *the same* stimulus $\epsilon I(t)$, and to record spike times in raster plots. Fig. 1 contains the results for cell 1 for two distinct sets of connection strengths. On the left is the *feedforward case*, with $a_{\rm ff} = 1$ and $a_{\rm fb} = 0$: After a brief transient, every trial (*i.e.* every initial state) evolves to produce identical spike times. This is a signature of reliability. With $a_{\rm fb} = 0$, the presence of cell 2 is irrelevant; our results are thus consistent with [3, 4]. On the right is the *positive feedback case*, where $a_{\rm ff} = 1$ and $a_{\rm fb} = 1.5$:

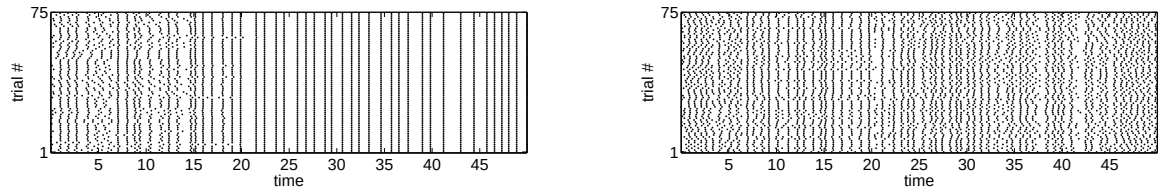

FIG. 1: Raster plots. In each experiment, the results of 75 trials are shown, and dots are placed at spike times of cell 1 (with each trial corresponding to one row). **Left:** feedforward network ($a_{\rm ff} = 1$, $a_{\rm fb} = 0$), exhibiting identical spike times or reliability. **Right:** Positive feedback ($a_{\rm ff} = 1$, $a_{\rm fb} = 1.5$) with unreliable responses.

The plot shows that even though some spiking events are shared, there is no convergence to common spike times.

II. RANDOM ATTRACTORS

With $I(t)$ taken to be realizations of white noise, we treat (1) as a stochastic differential equation (SDE), and its solutions as *random dynamical systems* (RDS). We review below some relevant mathematical facts and discuss their interpretations.

Review of RDS theory [9]: Consider the SDE

$$dx_t = a(x_t)\ dt + b(x_t)\ dB_t\ , \tag{2}$$

where B_t is a standard Brownian motion. We assume that the steady-state statistics of x_t are governed by a stationary probability measure μ which has a density (μ can be found by solving the Fokker-Planck equation). By a very general theorem, the solution of (2) has a representation as an RDS: Associated with almost every sample Brownian path ω is a family of diffeomorphisms (i.e. smooth invertible transformations) of the phase space $\{F_{s,t;\omega}, s < t\}$ with the property that for every point x in the phase space, if $x_s = x$, then $F_{s,t;\omega}(x) = x_t$ gives the solution to the SDE at time t.

Thinking of the process as starting from $t = -\infty$, we obtain a family of *sample measures* $\{\mu_\omega\}$ which are conditional measures of μ given the history of the Brownian path up to time 0. That is, μ_ω describes what one sees at $t = 0$ given that the system has experienced the perturbations defined by the realization of Brownian motion ω for $t < 0$. This property can also be expressed by

$$(F_{-t,0;\omega})_*\mu \to \mu_\omega \quad \text{as} \quad t \to \infty \tag{3}$$

where $(F_{-t,0;\omega})_*\mu$ is the measure obtained by transporting μ forward by $F_{-t,0;\omega}$. Finally, the family $\{\mu_\omega\}$ is invariant in the sense that $(F_{0,t;\omega})_*(\mu_\omega) = \mu_{\sigma_t(\omega)}$ where $\sigma_t(\omega)$ is the time-shift of the sample path ω by t.

Interpretation: For us, $x_t = (\theta_1(t), \theta_2(t))$, our phase space is $\mathbb{S}^1 \times \mathbb{S}^1$, and each ω corresponds to a stimulus $I(t), t \in (-\infty, \infty)$. If our initial distribution is given by a probability density ρ and we apply the stimulus ϵI, then the distribution at time t is $(F_{0,t;\omega})_*\rho$. For t sufficiently large, one expects in most situations that $(F_{0,t;\omega})_*\rho$ is very close to $(F_{0,t;\omega})_*\mu$, which by (3) is essentially given by $\mu_{\sigma_t(\omega)}$. The time-shift by t of ω is necessary because by definition, μ_ω gives the conditional distribution of μ at time 0.

Fig. 2 shows some snapshots of $(F_{0,t;\omega})_*\rho$, which, in the latter panels (where $t \gg 1$), approximate $\mu_{\sigma_t(\omega)}$. The initial density ρ (prior to the presentation of ϵI) is the steady state of the network under weak (amplitude 0.01) white noise [10]. As in Fig. 1, results for two distinct cases are shown, feedforward in the top row and positive feedback in the bottom row.

Two relevant results: Lyapunov exponents (LE) measure the exponential rates of separation of nearby trajectories in a dynamical system [11]. The value of the largest LE, $\lambda_{\max}$, contains a great deal of information about the system: A positive $\lambda_{\max}$ for a large set of trajectories is synonymous with chaos, while the presence of stable equilibria is characterized by $\lambda_{\max} < 0$. As in deterministic systems, LE for RDS are well defined, and they are *nonrandom*, i.e. they do not depend on ω.

THEOREMS. *The setting is as above; μ has a density.*
(1) **(Random sinks)** [12] *If $\lambda_{\max} < 0$, then with probability 1, μ_ω is supported on a finite set of points.*
(2) **(Random strange attractors)** [13] *If $\lambda_{\max} > 0$, then with probability 1, μ_ω is a random SRB measure.*

SRB measures are special invariant measures that describe the asymptotic dynamics of chaotic *dissipative* dynamical systems. They live on unstable manifolds, which are families of curves, surfaces etc. that wind around in a complicated way in the phase space [11].

Consequences for reliability and unreliability: Since reliability means the system's reaction to a stimulus is independent of its initial state, it corresponds to a random fixed point, or $\lambda_{\max} < 0$, as observed in [3, 4]. Complicated sets generated by unreliable dynamics have also been numerically observed before [5]. We point out here that the characterization of unreliable dynamics by SRB measures has two important consequences. First, the very distinctive geometries of random sinks and SRB measures provide a dichotomy between reliability and unreliability that is easy to recognize in simulations (see Fig. 2). Second, because the μ_ω are singular (even though μ has a density), different initial conditions are attracted to a low-dimensional set that depends on the stimulus history. This implies that even in unreliable dynamics,

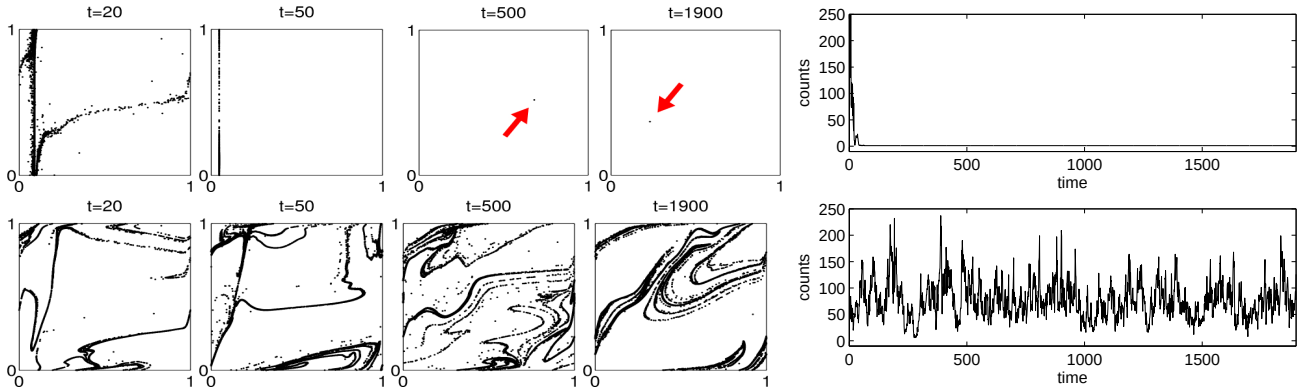

FIG. 2: States of 50, 000 initial conditions evolved for 1900 units of time. Snapshots at various times of sample measures in response to a single realization of the stimulus are shown. (Top) *Feedforward network*: the states converge to a random fixed point. (Bottom) *Feedforward network*: the states converge to random strange attractor. (Far right) Number of grid elements in a 30×30 grid needed to cover 90% of the trajectories are plotted as a function of time; it shows in particular that pictures of random SRB measures with their characteristic geometry, though fluctuating in time, are persistent.

the responses are highly structured and far from uniformly distributed, a fact illustrated in Fig. 1(right).

Observe that since $\lambda_{\max}$ is nonrandom, reliability is independent of the realization ω once stimulus amplitude is fixed.

III. CONNECTION STRENGTHS, STIMULUS AMPLITUDE AND RELIABILITY

There are many ways to quantify the degree of reliability. In view of the results in Sec. II, we will use $\lambda_{\max}$. Fig. 3 shows $\lambda_{\max}$ as a function of feedback strength $a_{\rm fb}$ and stimulus amplitude ϵ. Regions of reliability and unreliability are clearly visible. A closer examination of this plot reveals many interesting phenomena that beg for explanations:

(A) For a fixed value of $a_{\rm fb}$, how does increasing ϵ affect reliability? Fig. 3 shows there is no simple answer. When $a_{\rm fb} = 0$, increasing ϵ makes $\lambda_{\max}$ more negative (a result consistent with [4]), while at $a_{\rm fb} \approx 1.4$, $\lambda_{\max}$ increases with ϵ. As if to confuse matters further, for $a_{\rm fb} \in (1.5, 2.0)$, the system is reliable for small ϵ, unreliable as ϵ gets larger.

(B) Next we fix a value of ϵ, say around $\epsilon = 1.5$, and ask how reliability properties vary with $a_{\rm fb}$. Notice that $\lambda_{\max}$ attains its minimum at $\epsilon = 0$, i.e. the purely feedforward network is the most reliable of all. For relatively small values of $|a_{\rm fb}|$, negative feedback is more reliable than positive feedback, and the system is unambiguously unreliable for a range of larger positive $a_{\rm fb}$-values.

(C) We focus on the small-input region $\epsilon \approx 0$, and observe the "triple point" near $a_{\rm fb} = 1.4$, where a small-amplitude stimulus has the largest impact on $\lambda_{\max}$. To explore why this configuration is especially vulnerable, we study the zero-input system to look for clues near $a_{\rm fb} = 1.4$. Fig. 4(a) shows the smaller Lyapunov exponent $\lambda_{\min}$ for the system with $\epsilon = 0$ as a function of $a_{\rm fb}$. One sees that $\lambda_{\min} = 0$ up to about $a_{\rm fb} = 1.4$, close to where the triple point occurs. There it turns negative abruptly and begins to decrease [14].

Analogs of Figs. 3 and 4(a) (not shown) for $a_{\rm ff} = 1.5$ produce very similar results. The critical value of $a_{\rm fb}$ differs, but there is a similar correspondence between a triple point in the $\lambda_{\max}$-picture and the transition in $\lambda_{\min}$ for the zero-input system, suggesting that this is a general phenomenon.

IV. GEOMETRIC EXPLANATIONS

We review some well known facts from dynamical systems theory: Chaos often results from stretch-and-fold actions; prototypical examples are Smale's horseshoe and Hénon's attractor. Phase-space stretching is essential for

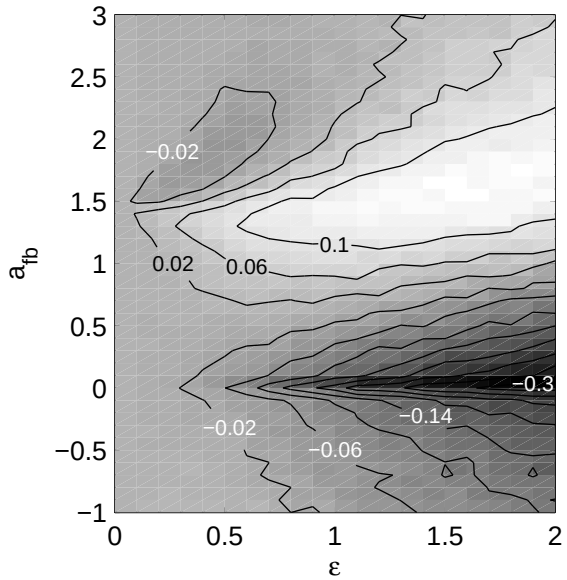

FIG. 3: Larger Lyapunov exponent $\lambda_{\max}$ as function of $a_{\rm fb}$ and ϵ (with fixed $a_{\rm ff} = 1$, $\omega_1 = 1$, $\omega_2 = 1.1$).

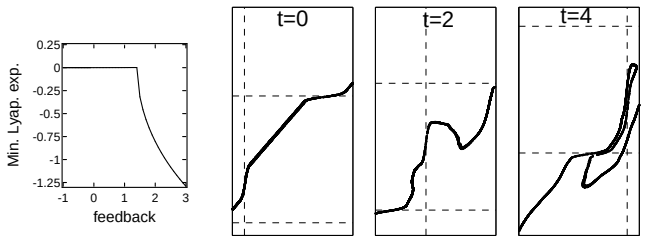

(a) (b)

FIG. 4: (a) Smaller Lyapunov exponent $\lambda_{\min}$ for the *unforced* ($\epsilon = 0$) network, as function of $a_{\rm fb}$. (b) Folding action near limit cycle at $a_{\rm fb} = 1.4, \epsilon = 1.5$: at $t = 0$, the curve shown (with ends identified) is the limit cycle; the second and third curves are images of the first, lifted to $\mathbb{R}^2$. Dotted lines indicate the integer grid over the plotted region.

the creation of positive Lyapunov exponents, but it alone does not imply the existence of strange attractors or SRB measures: Expansion is necessarily compensated by contraction in some other directions or regions, and contraction leads easily to stable equilibria or sinks. There is tension between these forces; in general, positive exponents prevail if there is a sustained expansion in roughly identifiable directions. We now apply this thinking to the context of Sec. III.

The 2-cell feedforward network is never unreliable: In Equation (1) with $a_{\rm fb} = 0$ and any ϵ, if $\theta_1(0) = \bar\theta_1(0)$, then $\theta_1(t) = \bar\theta_1(t)$ for all t. Geometrically, this says that the maps $F_{s,t;\omega}$ in Sec. II leave invariant the family of circles $\{\theta_1 = c\}$ in the torus $\mathbb{S}^1 \times \mathbb{S}^1$. Since such a geometry precludes folding of any kind, no chaotic behavior is possible.

Role of unforced dynamics in unreliability: The flow generated by (1) with $\epsilon = 0$ is a perturbation (due to the coupling) of a linear flow with frequencies ω_1 and ω_2. Typically, the perturbed flow is either quasi-periodic or possesses limit cycles. Fig. 4(a) tells us that quasi-periodicity dominates for $a_{\rm fb} < 1.4$, beyond that limit cycles prevail. In the region of $a_{\rm fb} > 1.4$ explored, we find that there is a single cycle of period ≈ 1 to which all points in the phase space are drawn. Fig. 4(b) shows how this cycle is folded by the maps $F_{0,t;\omega}$ for a randomly chosen stimulus, setting the stage for the formation of strange attractors.

It has been shown that limit cycles facilitate folding by providing clear directions of potential expansion and contraction. Quasi-periodic dynamics do not provide such preferred directions. In order for the folding to occur, however, one must first "break" the cycle.

Why the triple-point? Strongly attractive cycles are harder to break and are likely to fold only when a stronger stimulus is applied. Weakly attractive cycles fold more readily. Folding occurs, in fact, before a cycle is born, as soon as phase points are attracted to a band. These observations explain why the onset of phase-locking in the zero-input system coincides with $\lambda_{\max} > 0$ for weak ϵ. For $a_{\rm fb} \gtrsim 1.5$, where the cycle is more robust ($\lambda_{\min}$ is more negative), the coupled system acts as a single – and hence reliable– phase oscillator, explaining the small "island" of $\lambda_{\max} < 0$ seen there.

The ideas above come from the Wang-Young theory of periodically kicked limit cycles, a rigorous theory explaining how small folds created by kicks and amplified by shear lead to the formation of strange attractors [15]. To determine to what extent similar mechanisms are at work in Eq. 1 requires further analysis.

Conclusion. We have demonstrated, via numerics and mathematical reasoning, the assertions stated in the Introduction. Our main findings have implications for larger networks and for the encoding of stimuli.

K.L. and E.S-B. hold NSF Math. Sci. Postdoctoral Fellowships and E.S-B. a Burroughs-Wellcome Fund Career Award; L-S.Y. is supported by a grant from the NSF.

[1] L. Glass & M. Mackey. *From Clocks to Chaos* (Princeton U. Press, 1988); A. Pikovsky, M. Rosenblum, & J. Kurths, *Synchronization* (Cambridge U. Press, 2001).

[2] H. Bryant & J. Segundo, J. Physiol. **260** 279 (1976); Z. Mainen & T. Sejnowski, Science **268** 1503 (1995).

[3] H. Nakao et al., Phys. Rev. E **72** 026220 (2005); C. Zhou & J. Kurths, Chaos **13** 401 (2003).

[4] J. Teramae & D. Tanaka, Phys. Rev. Lett. **93** 204103 (2004); J. Ritt, Phys. Rev. E **68** 041915 (2003); K. Pakdaman & D. Mestivier, Phys. Rev. E **64** 030901 (2001); K. Pakdaman & D. Mestivier, Phys. D **192** 123 (2004).

[5] E. Kosmidis & K. Pakdaman, J. Comp. Neurosci. **14** 5 (2003); D. Goldobin & A. Pikovsky, Phys. Rev. E **71** 045201 (2005).

[6] A. Winfree, *Geometry of Biological Time* (Springer, 2001); D. Taylor & P. Holmes, J. Math. Biol. **37** 419 (1998).

[7] A. Winfree, J. Math. Biol. **1** 73 (1974); G.B. Ermentrout & N. Kopell, SIAM J. Math. Anal. **15** 215 (1984); E. Brown, J. Moehlis, & P. Holmes, Neural Comput. **16** 673 (2004).

[8] G.B. Ermentrout, Neural Comp. **8** 979 (1996).

[9] L. Arnold, *Random Dynamical Systems*, (Springer, 2003); P. H. Baxendale, in Progr. Probab. **27** (Birkhäuser, 1992).

[10] This is based on the presumption that the system is intrinsically noisy. To clarify the source of unreliability in our model, the noise is turned off when $\epsilon I(t)$ is presented; leaving this weak noise on has little effect.

[11] J.-P. Eckmann & D. Ruelle, Rev. Mod. Phys. **57** 617 (1985).

[12] Y. Le Jan, Z. Wahr. Verw. Geb. **70** (1985)

[13] F. Ledrappier & L.-S. Young, Probab. Th. & Rel. Fields **80** 217 (1988).

[14] Closer examination reveals that $\lambda_{\min}$ is, in fact, negative on some very tiny intervals for $a_{\rm fb} < 1.4$.

[15] Q. Wang & L.-S. Young, Comm. Math. Phys. **225** 275 (2002) & Comm. Math. Phys. **240** 509 (2003); see also K. K. Lin, SIAM J. Appl. Dyn. Sys. **5** 179 (2006) and D. Goldobin & A. Pikovsky, Phys. Rev. E **73** 061906 (2006).